
LLaMP: Large Language Model Made Powerful for High-fidelity Materials Knowledge Retrieval and Distillation

Yuan Chiang^{1,2*}, Elvis Hsieh¹, Chia-Hong Chou³, Janosh Riebesell^{2,4}

¹University of California, Berkeley, ²Lawrence Berkeley National Laboratory,

³Foothill College, ⁴Cavendish Laboratory, University of Cambridge, UK

Abstract

Reducing hallucination of Large Language Models (LLMs) is imperative for use in the sciences, where reliability and reproducibility are crucial. However, LLMs inherently lack long-term memory, making it a nontrivial, *ad hoc*, and inevitably biased task to fine-tune them on domain-specific literature and data. Here we introduce **LLaMP**, a multimodal retrieval-augmented generation (RAG) framework of hierarchical reasoning-and-acting (ReAct) agents that can dynamically and recursively interact with computational and experimental data on [Materials Project \(MP\)](#) and run atomistic simulations via high-throughput workflow interface. Without fine-tuning, LLaMP demonstrates strong tool usage ability to comprehend and integrate various modalities of materials science concepts, fetch relevant data stores on the fly, process higher-order data (such as crystal structure and elastic tensor), and streamline complex tasks in computational materials and chemistry. We propose a simple metric combining uncertainty and confidence estimates to evaluate the self-consistency of responses by LLaMP and vanilla LLMs. Our benchmark shows that LLaMP effectively mitigates the intrinsic bias in LLMs, counteracting the errors on bulk moduli, electronic bandgaps, and formation energies that seem to derive from mixed data sources. We also demonstrate LLaMP’s capability to edit crystal structures and run annealing molecular dynamics simulations using pre-trained machine-learning force fields. The framework offers an intuitive and nearly hallucination-free approach to exploring and scaling materials informatics, and establishes a pathway for knowledge distillation and fine-tuning other language models. Code and live demo are available at <https://github.com/chiang-yuan/llamp>.

1 Introduction

The generation of convincing yet unreliable information poses a pressing challenge to large language model (LLMs), particularly to their application in the sciences. LLMs are prone to hallucination—providing outright false information with high confidence [1, 37]. This issue is particularly concerning for knowledge-intensive tasks, where users rely on chatbots and other AI systems to provide accurate guidance [18]. LLMs often lack up-to-date factual knowledge on topics outside their training data, requiring rigorous verification against trusted external sources [24]. In the scientific community, where the integration of insights and data accuracy is already complex, the proliferation of generative models may exacerbate the risk of misinformation. This trend accentuates the importance of scrutinizing and ensuring the reliability of information sources.

*Correspondence to: cyrusyc@berkeley.edu

Current approaches to enhance LLM accuracy in domain-specific knowledge often involve fine-tuning pre-trained models [7, 11] or tailored prompt engineering techniques [38, 41]. While these models are easy to deploy, they suffer from diminished reproducibility and data adherence due to the absence of a memory base, untraceable fine-tuning history, or opaque extraction processes. Even though fine-tuning can encode a certain amount of domain-specific knowledge into LLMs, it is constrained by scalability and intrinsic memory capacity. Fine-tuned LLMs struggle to retain in the long term the knowledge they were trained on as the training progresses, nor can they be aware of the up-to-date events and data beyond pre-training. Prompt engineering, while effective, also compromise the generalizability, thus limiting the overall power and flexibility of LLMs. Therefore, a more sensible approach involves equipping LLMs with external data sources, allowing them to generate holistic responses via few-shot adaptation to factual information [18] that can reliably support real-world scientific research and decision-making.

In this work, we propose LLaMP, a multimodal retrieval-augmented generation (RAG) framework leveraging hierarchical reasoning-and-acting (ReAct) agents to interact with Materials Project (MP), arXiv, Wikidpeia, and atomistic simulation tools. The framework serves as a safeguard against LLM hallucination and grounds them on high-fidelity material informatics derived from various sources, including computational data from quantum-mechanical first-principles calculations and expert-curated material synthesis recipes [16], and further enables the possibility of language-driven simulations. Through hierarchical planning of multiple ReAct agents [39], we demonstrate that LLaMP not only can correctly retrieve higher-order materials data such as tensors and 3D crystal structures but also can combine different modalities to perform complex, knowledge-intensive inferences and operations essential for real-world research applications.

We summarize our contributions as follows:

- We implement a multimodal RAG framework of hierarchical ReAct agents that can dynamically and recursively interact with Materials Project to ground LLMs on high-fidelity materials informatics.
- We propose a metric to statistically evaluate the self-consistency and confidence of the LLM responses for settings that require high precision and reproducibility.
- We evaluate the performance of LLaMP and vanilla LLMs on the prediction of various material properties, including bulk moduli, electronic bandgaps, formation energies, and magnetic orderings.
- Real-world materials science applications including inorganic synthesis and crystal structure generation and editing are demonstrated.
- We augment LLaMP with high-throughput atomistic simulation workflow and pre-trained universal machine learning force fields to further lower the barrier of computational materials and chemistry.

2 Background

Materials Project (MP) The Materials Project is a multi-institution effort to explore and compute the properties of all known inorganic materials [14] and molecules [31]. The initiative leverages high-throughput electronic structure calculations [17, 30] based on density functional theory (DFT), providing large-scale open-source database and analysis algorithms, with the ultimate goal to drastically reduce the time and cost required for materials discovery by focusing experiments on the promising candidates from computational screening. Most of the atomic structures are selected from the Inorganic Crystal Structure Database (ICSD) [40] and undergo standardized relaxation procedures, followed by post-processing or additional calculations for higher-order material properties such as electron and phonon bandgaps, elastic tensors, dielectric tensors, and more. MP provides these calculated material properties through API endpoints.

Natural language processing (NLP) in science NLP has found extensive application in extracting valuable information from scientific publications, with notable instances involving text-to-text or more recent image-to-text summarization techniques [11, 29, 34]. For summarizing crystal structures in textual form, Ganose and Jain [9] introduced the *robocrystallographer*, a toolkit designed for the analysis and generation of descriptions for crystalline materials. Their method condenses atomic

structures into descriptive JSON representations that encompass coordination statistics, connectivity motifs, geometric features, and dimensionality. MP leverages robcystallographer to generate human-level descriptions for 130K compounds which are accessible through MP website and API.

3 Related Work

Prompting and fine-tuning in domain science Prompt-based methods have been used as effective tools for automating data extraction process from the literature. Polak and Morgan [28] employ a prompt workflow to extract the cooling rates of metallic glasses and yield strengths of high entropy alloys. Zheng et al. [41] implement a ChatGPT metal-organic framework (MOF) synthesis assistant through embedding and searching on preselected papers. StructChem [27] leverage step-by-step reasoning, and iteratively refining results to solve college-level chemistry questions. Yang et al. [38] use GPT-4 to extract experimentally measured bandgaps to train a graph neural network for accurate bandgap prediction from crystal structures. Despite the success in the specific data extraction tasks, prompt-based methods face challenges in reproducibility when the used prompts are fine-grained to work for specific edge cases. They are also still prone to hallucination and less generalizable to combine different data sources due to the deliberately designed prompt.

Several other knowledge-grounded, domain-specific language models lean on the fine-tuning approach against pre-selected data and literature. For instance, ChemGPT [8] involves fine-tuning GPT-neo on self-referencing embedded strings (SELFIES) representations of small molecules. Jablonka et al. [13] demonstrated GPT-3 fine-tuned against online corpora could outperform purpose-trained models on classification, regression, and inverse design of high-entropy alloys and molecules. Dagdelen et al. [7] fine-tuned GPT-3 on ~ 500 prompt-completion pairs to enhance LLM’s capability to extract useful information on materials chemistry from text paragraphs. However, the fine-tuned models without augmentation inherently lack awareness of the up-to-date results and any data only available after their training. Moreover, fine-tuned LLMs still suffer from limited memory retention and are prone to forget during continual training [35].

LLM function calling and tool usage An emerging class of LLM applications, including this work, take advantage of LLM text completion and instruction following capability for function calling. This approach extends LLMs with expert-curated tools to improve the quality of control for downstream applications. Coscientist [3] combines tools such as search engines, Python, and document index for autonomous chemical research. ChemCrow [23] gathers multiple molecule and safety tools to enhance organic chemistry experiment and molecule design.

However, most prior works adopt *flat planning* strategy, where a single agent accesses all the available tools, resulting in a lack of self-correcting tool usage capabilities. This often leads to premature reasoning stop and summarization when the agent encounters tool usage errors. We mitigate this through *hierarchical planning* of multiple ReAct agents (see Section 4).

4 Method

Retrieval-augmented generation (RAG) While LLMs and generative pre-trained transformers have demonstrated the capability to store factual knowledge in model parameters, their ability to accurately access and manipulate precise information is limited. Deliberate prompting does not entirely resolve this problem and, in fact, can make models overly sensitive to input requests and induces serious hallucinations. To address these challenges, Lewis et al. [19] proposed the RAG framework, which significantly mitigates these problems through the retriever-generator paradigm. The original RAG framework has two components: (i) a retriever $p_\eta(z|x)$ with parameters η that returns top-K documents given the input text sequence x and (ii) a generator $p_\theta(y_i|x, z, y_{1:i-1})$ with parameters θ that generates the current output text sequence y based on the context of input sequence x , the retrieved document z , and the previous output sequences $y_{1:i-1}$ [19]. The retriever and generator are here replaced by LLMs, and an intermediate data retrieval step is introduced: API function calls to Materials Project, arXiv, and Wikipedia are executed to retrieve consistent and reliable data, which is then parsed or filtered by LLMs to generate text or JSON responses.

Reasoning and acting (ReAct) One-shot generation often falls short in delivering optimal performance for numerous knowledge-intensive reasoning tasks (*e.g.* HotpotQA, Fever) [39]. In an effort to enhance performance, Wei et al. [36] introduced the chain-of-thought (CoT) framework, which

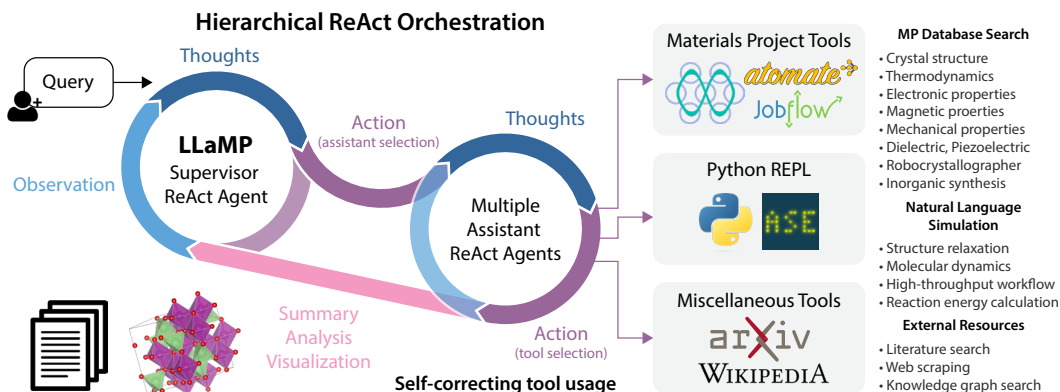


Figure 1: Hierarchical ReAct agent planning in LLaMP. Two levels of agents are deployed using a standardized LangChain interface. Supervisor ReAct agent oversees assistant ReAct agents at the bottom-level, each equipped with distinct toolkits and data/document stores to accomplish various tasks, including high-fidelity materials information retrieval, atomistic modeling and simulations, and literature search. For detailed example, check Figure A.1.

encourages language models to engage in reasoning before generating a response. While successful in boosting performance, CoT is susceptible to hallucinations arising from the generated thoughts. Here we adopt ReAct [39] to augment the agent’s action space \mathcal{A} with a language space \mathcal{L} to create an expanded action space $\hat{\mathcal{A}} = \mathcal{A} \cup \mathcal{L}$. This expanded action space empowers the agent to take action $\hat{a}_t \in \mathcal{L}$ in language space that allows reasoning over context and tool results. The action \hat{a}_t functions as a *thought*, synthesizing valuable information by reasoning over the existing context c_t and updating the context $c_{t+1} = (c_t, \hat{a}_t)$ for future actions [39]. ReAct implementation for assistant agents is essential in improving the hit rate of function calls and the quality of API responses by few-shot refinement from the error messages.

Hierarchical orchestration To manage heterogeneous data sources and diverse types of queries, we introduce hierarchical ReAct agent planning, featuring the supervisor ReAct agent overseeing assistant ReAct agents (Figure 1). This design offers three major advantages over flat planning commonly implemented in previous works [3, 23]. Firstly, the supervisor agent acts as a router and decision-maker, handling abstract logic between user requests and assistant agents, thereby enhancing the robustness and interpretability of the final response. Secondly, supervisor agents can integrate different sources of data parsed via assistant agents, enhancing the completeness of the final response. Thirdly, the process of function calling necessitates LLMs to assimilate API schemas, a task that can impede efficiency by consuming large portion of the context window and accelerating the depletion of API tokens. By delegating multiple functions to assistant agents, we effectively reduce the total number of required tokens and circumvent unnecessary schema parsing. Simultaneously, adherence to API schemas is improved since LLMs increasingly struggle to comply if said schemas approach significant fractions of the context window.

Self-consistency of response (SCoR) When LLMs are integrated in scientific workflows and deployed in high-stakes settings (*i.e.* self-driving labs), it is important for these models to have consistent and predictable behaviors [21]. For numeric knowledge retrieval tasks, we first define *precision* as the sample standard deviation of n valid responses from N trials: $\text{Precision} = \hat{\sigma}/\sqrt{n} \geq 0$ to estimate the uncertainty of the model for a given query, where $\hat{\sigma}$ is the standard deviation of all valid responses. We then formally define a transformation that maps precision to $[0, 1]$. Given the precision of the model, the *coefficient of precision* is defined as

$$\text{CoP} = \exp(-\text{Precision}) = \exp\left(-\frac{\hat{\sigma}}{\sqrt{n}}\right) \in (0, 1]. \quad (1)$$

Over the total N trials, the *confidence* of a model in generating n valid responses given a query is straightforwardly defined as the probability of valid response n/N . We finally define *self-consistency of response* as the product of CoP and Confidence:

$$\text{SCoR} = \text{CoP} \times \text{Confidence} \in [0, 1]. \quad (2)$$

The limit of $\text{SCoR} = 1$ is reached when the model yields the same response to a given query every time. At the limit of $\text{SCoR} = 0$, the model is either very inconsistent (with large variance across the responses) or very reluctant (with low confidence) to answer the query. Despite the simplicity in definition, SCoR effectively reflects the reproducibility and practical usability of the method, which is important when the method is incorporated into broader systems where the stable and expected behaviors are prioritized.

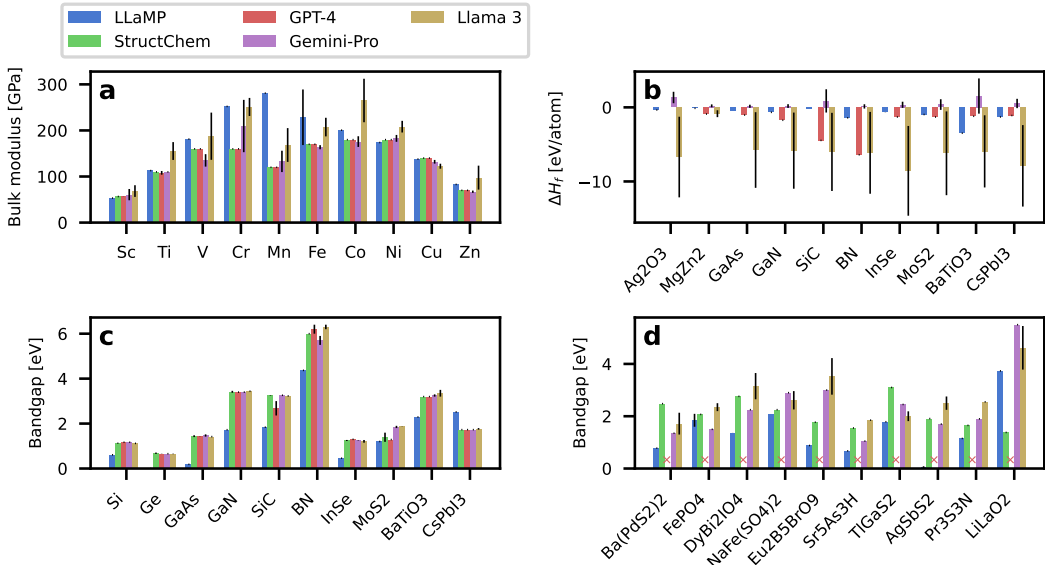


Figure 2: LLaMP RAG responses vs LLM intrinsic knowledge on material properties. (a) Bulk moduli, K , of 3d transition metals. (b) Formation energies, ΔH_f , of common compounds. (c) Electronic bandgaps, E_g , of common intrinsic semiconductors. (d) Electronic bandgaps of multi-element (ternary or quaternary) materials. Missing predictions are marked by cross symbols. All LLaMP results use GPT-4 as backend language provider.

5 Experiments

5.1 Multimodal ReAct augmentation

Materials design often involves multi-objective property optimization. These properties span a Pareto front where optimizing one factor incurs deterioration in others. To succeed in such tasks, combining different modalities of materials properties is necessary. LLaMP achieves this through the hierarchical orchestration of multiple ReAct agents [39]. For the example question “*What’s the stiffest material with the lowest formation energy in Si-O system?*” (Figure A.1), when a query requires multimodal information and compound logic, the supervisor agent decomposes the query into multiple subtasks, delegates them to assistant agents (MPThermoExpert and MPElasticityExpert) for information retrieval, and in the final stage of reasoning integrates information from both modalities, drawing on the context in episodic memory retrieved from the assistant agents. This enables LLaMP to achieve various tasks step-by-step by combining multiple data sources (*e.g.* crystal structures, thermodynamic, mechanical, magnetic properties, and more listed in Figure 1) in a single query. In fact, we found that flat planning implementation struggles to accomplish tool usages and RAG because the single agent sees too much information at once and often fails to follow the API schema (see Section 4 for details).

5.2 Performance benchmarks

Response quality and consistency We assess the responses of LLaMP, StructChem [27], and vanilla LLMs (gpt-4, llama3-8b, gemini-pro) on the bulk modulus, formation energy, and bandgap of selected materials (Figure 2, Table 1). We measure the performance with several metrics

Table 1: Performance metrics of LLaMP and LLM baselines on the prediction of material properties. The metrics from left to right are precision (sample standard deviation), coefficient of precision (CoP), confidence, self-consistency of response (SCoR), and mean absolute error (MAE), where Materials Project values are taken as ground truth. All the tabulated values are the average metrics for multiple materials. All LLaMP and StructChem results use GPT-4 as backend language provider.

	Bulk Modulus K (GPa)					Formation Energy ΔH_f (eV)				
	Precision	CoP	Confidence	SCoR	MAE	Precision	CoP	Confidence	SCoR	MAE
LLaMP	2.698	0.900	1.000	0.900	14.574	0.001	0.999	0.950	0.949	0.001
StructChem	0.000	1.000	0.400	0.400	41.017	-	-	0.000	0.000	-
GPT-4	0.186	0.910	1.000	0.910	41.224	0.000	1.000	0.225	0.250	1.680
Gemini-Pro	6.065	0.169	1.000	0.169	43.429	0.371	0.724	1.000	0.724	1.549
Llama 3	11.222	0.010	1.000	0.010	41.874	2.540	0.137	0.950	0.135	5.536

	Electronic Bandgap E_g - Common (eV)					Electronic Bandgap E_g - Multi-element (eV)				
	Precision	CoP	Confidence	SCoR	MAE	Precision	CoP	Confidence	SCoR	MAE
LLaMP	0.000	1.000	1.000	1.000	0.000	0.016	0.985	0.933	0.918	0.178
StructChem	0.017	0.984	1.000	0.984	0.986	0.000	1.000	0.200	0.200	0.973
GPT-4	0.037	0.966	1.000	0.966	0.943	-	-	0.000	0.000	-
Gemini-Pro	0.025	0.976	1.000	0.976	1.012	0.000	1.000	0.333	0.333	0.906
Llama 3	0.025	0.975	1.000	0.975	1.067	0.196	0.831	0.867	0.698	1.106

(Precision, CoP, SCoR, MAE) reported in Table 1. SCoR estimates the consistency and usability of the LLM agents (Section 4). We argue that any useful LLM agents to be included in the scientific workflow should have high SCoR and low error on the materials properties. Our results indicate that LLaMP significantly excels in these metrics. Even with extensive prompting strategies, StructChem [27] fails to answer correctly without necessary domain knowledge. Its refinement process, which is intended to validate reasoning and data, frequently results in a high refusal rate, as the model cannot verify its outputs.

We found most of the popular LLMs are strongly anchored to the low-fidelity values that are easily accessible online, with in particular Cr, Mn, Fe largely deviating from MP theoretical calculations in bulk moduli of transition metals experiment. Interestingly, Llama 3-8b usually cites spurious reference in the responses but occasionally agrees with MP values. It also exhibits the largest variance in the prediction and has lowest SCoR score (Table 1). LLaMP outperforms vanilla LLMs and reduces the MAE from around 40 to 14.57 GPa.

Vanilla language models tend to overlook the subtleties of domain-specific knowledge and display overconfidence in their intrinsic bias, which could be influenced by misleading data that appear more frequently and are more accessible. This is commonly referred to as the “tail knowledge problem” [15, 22]. Our results reveal that vanilla LLMs consistently fail to predict accurate formation energies, exhibiting poor scores for SCoR and MAE between 1.5 and 5.5 eV—a range impractical for material discovery where accuracy at the meV level is essential. This is not unexpected since accurate formation energy prediction requires the computation of multiple energetics (energies of the compound itself and its elemental constituents). In the bandgaps evaluation, we query 10 common compounds and 10 multi-element materials that are less commonly encountered in the literature. Vanilla LLMs perform surprisingly well on the bandgaps of common semiconductors (Figure 2c), with expected systematic deviation from MP values retrieved by LLaMP². This is likely due to the extensive literature on experimental semiconductor bandgaps, which have been studied and reported for decades. On the contrary, Figure 2d and Table B4.8 show that vanilla LLMs lack intrinsic knowledge of the bandgaps for the queried multi-element materials and exhibit low confidence or refuse to make predictions, whereas LLaMP could not only correctly retrieve the data with SCoR of 0.918 but also identify the bandgap of the stable form when multiple polymorphs are present.

High-fidelity and higher-order data retrieval The challenge for LLMs in excelling at knowledge- and data-intensive tasks is well-documented [6, 12, 21]. Figure 3 shows the prediction of LLaMP, GPT-3.5, and GPT-4 on the magnetic orderings and total magnetization of 800 materials randomly selected from all unary, binary, and ternary compounds in MP. Our result indicates

²Bandgaps calculated from generalized gradient approximation (GGA) functional are known to underestimate the experimental values by 40-50% [4]. Strategies to improve bandgap prediction at moderate or low computational cost will be included in MP in the future.

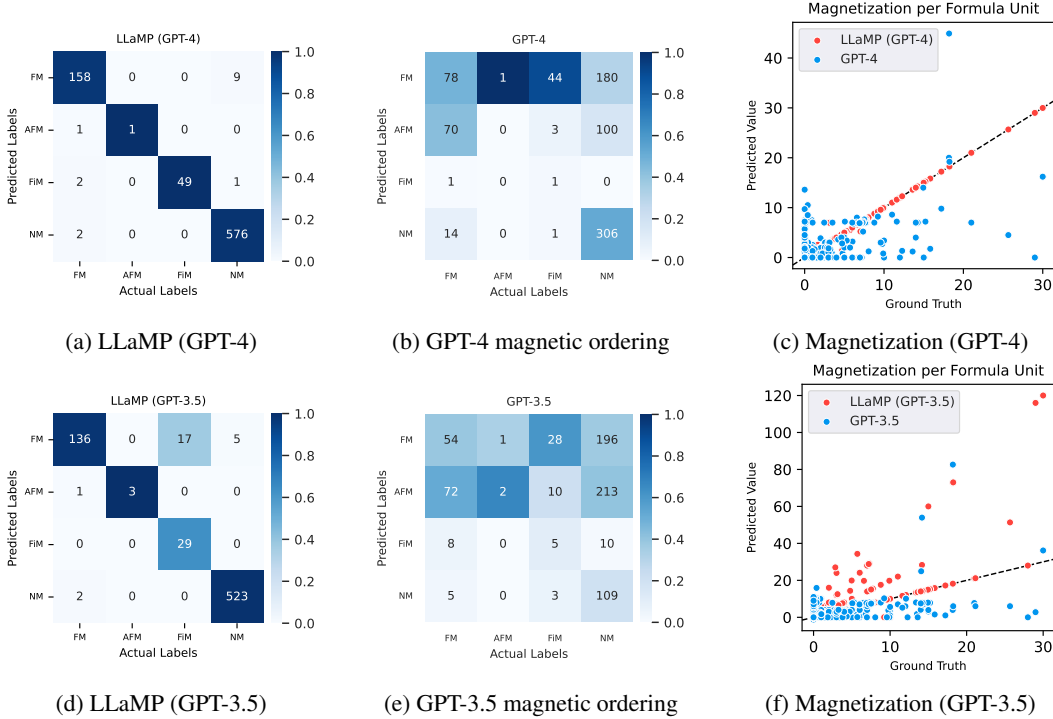


Figure 3: Prediction of LLaMP, GPT-3.5, and GPT-4 on magnetic orderings and total magnetization per formula unit of randomly selected materials. Confusion matrix presents the number of entries in each class. Colormap represents the percentage of correct classification.

that without RAG, vanilla LLMs suffer from hallucinations and misclassify the magnetic orderings of materials. LLaMP with GPT-4 as backend can counteract the intrinsic bias of GPT models, increasing the classification accuracy to 0.98 and R^2 of magnetization prediction to 0.992 (Table 2). We note that GPT-3.5 as backend, while effective for classification and other information retrieval tasks, struggles to distinguish total_magnetization from magnetization_per_formula_unit in magnetism API schema and often requests the wrong field and forgets to normalize the values. In the magnetic orderings queries, LLaMP with GPT-3.5 as backend fails to distinguish ferromagnetic (FM) and ferrimagnetic (FiM) orderings, while LLaMP with GPT-4 as backend gracefully separates the two classes (Figure 3a, d).

We further test the capability of LLaMP and LLMs for higher-order data (such as tensors, 3D crystal structures, curves). As shown in Table B4.2, GPT-3.5 hallucinates the values for the components in the elastic tensor of NaCl, with serious erroneous values such as $C_{11} = 289.2 \text{ GPa}$ —a significant deviation from DFT-calculated values (76 GPa). It also omits the values for $C_{22}, C_{33}, C_{55}, C_{66}$ and fails to represent the full elastic tensor in a matrix format, despite the query explicitly requesting the *full* elastic tensor. This highlights the limitation of intrinsic knowledge in LLMs to recall higher-order, more complex data for more comprehensive, holistic response.

Table 2: Prediction performance of LLaMP, GPT-3.5, and GPT-4 on magnetic orderings and magnetization. LLaMP with GPT-4 and GPT-3.5 as backend LLM are compared.

	Magnetic Ordering		Magnetization	
	Accuracy	F1	MAE	R^2
LLaMP (GPT-4)	0.98	0.89	0.045	0.992
GPT-4	0.48	0.26	1.611	-0.201
LLaMP (GPT-3.5)	0.96	0.88	1.896	0.407
GPT-3.5	0.23	0.18	1.988	-0.024

5.3 Real-world Applications

Inorganic synthesis recipes Empowered by the MP synthesis endpoint, LLaMP can extract synthesis recipes and summarize detailed step-by-step procedures grounded on real experimental papers with associated DOI references, as demonstrated in the example queries (Table B4.9 and B4.10). Vanilla GPT-3.5 gives a seemingly correct and verbose synthesis procedure for YMnO_3 in Table B4.9, inferring possible reaction pathways from two common oxides as precursors (Y_2O_3 and MnO_2). However, it pulls irrelevant lithium compounds (Li_2CO_3 and LiOH) into the recipe and overlooks the fact that metathesis reactions [20, 33] require less applied energy than high-temperature sintering, which relies on solid-state diffusion [25]. Vanilla GPT-3.5 also exhibits uncertainty about specific synthesis details, such as heating temperature, duration, cooling rate, *etc.*

Consider the example of LiFePO_4 presented in Table B4.10. Explicit instruction is provided: “Please provide a detailed step-by-step procedure and reference.” While GPT-3.5 does offer both a procedure and reference as asked, and the reference is indeed associated with a real paper, the paper itself contains no information about the synthesis procedure of LiFePO_4 . The procedure listed in Table B4.10 is dissociated from the title and is hallucinated from the pre-training corpus.

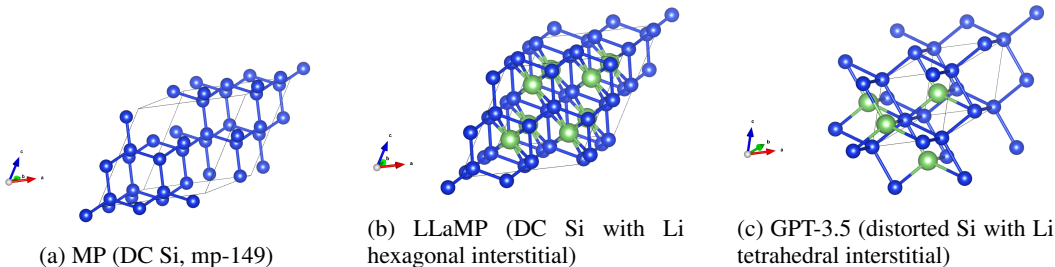


Figure 4: Generation and manipulation of crystal structures using LLMs to insert an additional lithium atom at the interstitial site in diamond cubic silicon structure. Blue: Si. Green: Li. Question-answer pairs are listed in Table B4.11. Additional atoms extended through bonds are visualized.

Table 3: Structural parameters of the generated crystals compared with diamond cubic (DC) silicon. From left to right are fractional coordinates of inserted Li atom $(x, y, z)_{\text{Li}}$, total cell volume V , average Si–Si bond lengths ℓ_{SiSi} , Si–Si–Si angles θ_{SiSiSi} , and Si–Li–Si angles θ_{SiLiSi} . GPT-4 refuses to response due to their safeguard against the lack of atomic structure information.

	$(x, y, z)_{\text{Li}}$	ℓ_{SiSi} (Å)	Error (%)	V (Å ³)	Error (%)	θ_{SiSiSi} (°)	Error (%)	θ_{SiLiSi} (°)
LLaMP	(0.5, 0.5, 0.5)	2.36	0.0	40.33	0.0	109.47	0.0	62.96
GPT-3.5	(0.5, 0.5, 0.5)	2.71	+15.0	67.05	+66.3	98.28	-10.2	67.69
GPT-4	-	-	-	-	-	-	-	-
DC Si (mp-149)		2.36		40.33		109.47		

RAG-assisted crystal generation and editing Fine-tuned LLMs for text-encoded atomistic information have shown the capability to generate stable crystals under the constraints of atomic positions and charges [10]. In this context, we delve into the examination and comparison of the crystal generation capabilities between LLaMP and GPT-3.5, without resorting to fine-tuning or tailored prompt messages in previous work. Figure 4 showcases the structures generated by LLaMP and vanilla GPT-3.5 without RAG, both instructed to *insert one lithium atom at the tetrahedral site of the diamond cubic silicon structure* (Table B4.11). Notably, both LLaMP and GPT-3.5 place an additional Li atom at fractional coordinate (0.5, 0.5, 0.5). However, the Si structure retrieved by LLaMP adheres to the MP convention, positioning two Si bases at (0.125, 0.125, 0.125) and (0.875, 0.875, 0.875). This causes the inserted Li atom to be *hexagonal interstitial* instead of *tetrahedral interstitial*.

GPT-3.5 locates the Li atom at the tetrahedral site given the “luckily chosen” Si bases at (0, 0, 0) and (0.25, 0.25, 0.25); however, the resulting cell volume and shape are highly distorted, and the Si–Si bond length and Si–Si–Si angle deviate significantly from the ground truth (Table 3), highlighting the limitations in the intrinsic encoding of LLMs for atomistic information and the challenges associated with zero-shot generation of crystal structures. In contrast, the LLaMP-retrieved MP

structure serves as a robust prior, anchoring the lattice parameters of the generated structure to the correct values.

Language-driven simulation LLaMP equipped with Python REPL and atomistic simulation workflow package `atome2` performs well out of the box for complex multi-step simulations using pre-trained universal machine learning force field MACE-MP-0 [2] through language instruction. As demonstrated in Appendix C.1 and Appendix C.2, LLaMP is able to follow multi-step instruction to fetch stable crystal structure from MP, generate a supercell of atomic structure, and run annealing molecular dynamics simulation with varying temperature from 300K to 800K and back to 300K. After the simulation is finished, LLaMP can read the simulation trajectories and plot the temperature profile over time (Appendix C.1).

6 Discussion

Robustness The hierarchical ReAct framework implemented here is essentially a graph of agents, or *language graph*, with one central node (supervisor) in connection with many satellite nodes (assistants). The implementation of ReAct for the assistant agents enables self-correcting tool usages and fortifies the robustness of data retrieval. As presented in Figure A.1c, `MPThermoExpert` initially misunderstood the schema at the first trial and filled in the `formula` field with `Si-O`, an invalid input but a valid one for chemical system (`chemsys`) field. The observation step (step 4) allows `MPThermoExpert` to handle exceptions and to refine the correct input fields after adaptation (step 6). Storing (Retrieving) question-answer and query-argument pairs to (from) vector databases could further reduce the number of trial-and-error steps, and the stored pairs can be used to refine foundation LLMs to improve function calling quality.

Limitation Sometimes LLMs misunderstand the description of schemas and therefore yield unexpected behaviors. For example, `sort_fields` argument allows sorting the returned documents in ascending order or descending order if the field is prefixed with `-`, but LLMs sometimes mistake the sign and sort in the opposite order. The correctness of LLaMP is also subject to the quality of theoretical prediction and the comprehensiveness of the data in MP. Other than the underpredicted bandgaps by GGA functional, MP’s ongoing effort to search all possible magnetic configurations is also not complete. Most of the existing calculations in MP start from high-spin ferromagnetic configurations, which may overlook many antiferromagnetic ground states below the current energy convex hull. While MP is one of the most comprehensive materials databases, the available crystal structures on MP are not exhaustive but continuously expanding [26]. Furthermore, Kohn-Sham DFT theory is insufficient in some cases, and a higher level of theory is needed. Currently LLaMP only supports a few `atome2` workflows with machine learning force fields and VASP calculations. More diverse electronic calculation methods and workflows will be supported in the future work.

Outlook LLMs and recent visual language models (VLMs) have demonstrated the promise to control robotics and guide autonomous chemical experiments [3, 5]. In the context of self-driving or autonomous labs [3, 32], LLM agents with multimodal data sources, sensors, and actors may improve their decision making and operation. For example, accurate formation energy data calculated from first principles, coupled with correct reaction energy calculations, can aid the identification of viable and faster reaction pathways and materials characterization that could be integrated into the autonomous lab feedback loop. The absence of access to a high-fidelity database through autonomous agents like LLaMP would escalate the number of trial-and-error iterations, making the scaling of self-driving laboratory prohibitively expensive and potentially hazardous.

Summary We present a hierarchical agentic framework, LLaMP, based on RAG and ReAct to extract and manipulate material informatics through few-shot generalization. By grounding thoughts and actions in high-fidelity information, LLaMP showcases the ability to integrate various modalities of material properties and perform logical inferences to accomplish assigned tasks, all without the need for fine-tuning. In essence, the proposed LangChain framework holds the potential to expand its applicability to multiple data sources, encompassing both theoretical computations and experimental data, and real-world laboratories by incorporating additional assistant agents for data retrieval and robot control. LLaMP functions as a knowledge-aware agent, empowering users to navigate and manipulate complex materials informatics. As new tools continue to emerge, there is an exciting avenue for further exploration to ascertain if this framework can effectively facilitate scientific hypothesis generation and guide data-driven experiments to test them.

Author Contributions

Yuan Chiang led, conceptualized, and designed the project, coded the Python backend and application frontend, ran the experiments (Section 5.1, Section 5.2, Section 5.3), and wrote the manuscript. Elvis Hsieh coded and ran the experiments (Section 5.2, Figure 3, Figure 2), compared the results with StructChem, and wrote the manuscript. Chia-Hong Chou coded the application frontend and web pages. Janosh Riebesell provided technical support on crystal visualization using `elementari` for the web application and revised the manuscript.

Acknowledgments

We appreciate the helpful discussion with Dr. Anubhav Jain and Dr. Karlo Berket at LBNL, and the early test and feedback from Dr. Matthew McDermott and Dr. Jordan Burns. Yuan Chiang acknowledges the support and advice from Prof. Mark Asta and the financial support from the Berkeley Fellowship from UC Berkeley and Taiwan-UC Berkeley Fellowship from the Ministry of Education in Taiwan.

We thank OpenAI for granting the API credits. This work was partly supported but not endorsed by the US Department of Energy, Office of Science, Office of Basic Energy Sciences, Materials Sciences and Engineering Division, under contract no. DE-AC02-05-CH11231 (Materials Project program KC23MP).

References

- [1] Y. Bang et al. A Multitask, Multilingual, Multimodal Evaluation of ChatGPT on Reasoning, Hallucination, and Interactivity, Nov. 2023. URL <http://arxiv.org/abs/2302.04023>. arXiv:2302.04023 [cs].
- [2] I. Batatia et al. A foundation model for atomistic materials chemistry, Dec. 2023. URL <http://arxiv.org/abs/2401.00096>. arXiv:2401.00096 [cond-mat, physics:physics].
- [3] D. A. Boiko, R. MacKnight, B. Kline, and G. Gomes. Autonomous chemical research with large language models. *Nature*, 624(7992):570–578, Dec. 2023. ISSN 1476-4687. doi: 10.1038/s41586-023-06792-0. URL <https://www.nature.com/articles/s41586-023-06792-0>. Number: 7992 Publisher: Nature Publishing Group.
- [4] P. Borlido et al. Exchange-correlation functionals for band gaps of solids: benchmark, reparametrization and machine learning. *npj Computational Materials*, 6(1):1–17, July 2020. ISSN 2057-3960. doi: 10.1038/s41524-020-00360-0. URL <https://www.nature.com/articles/s41524-020-00360-0>. Number: 1 Publisher: Nature Publishing Group.
- [5] A. Brohan et al. RT-2: Vision-Language-Action Models Transfer Web Knowledge to Robotic Control, July 2023. URL <http://arxiv.org/abs/2307.15818>. arXiv:2307.15818 [cs].
- [6] K. Cobbe et al. Training Verifiers to Solve Math Word Problems, Nov. 2021. URL <http://arxiv.org/abs/2110.14168>. arXiv:2110.14168 [cs].
- [7] J. Dagdelen et al. Structured information extraction from scientific text with large language models. *Nature Communications*, 15(1):1418, Feb. 2024. ISSN 2041-1723. doi: 10.1038/s41467-024-45563-x. URL <https://www.nature.com/articles/s41467-024-45563-x>. Publisher: Nature Publishing Group.
- [8] N. Frey et al. Neural Scaling of Deep Chemical Models, May 2022. URL <https://chemrxiv.org/engage/chemrxiv/article-details/627bddd544bdd532395fb4b5>.
- [9] A. M. Ganose and A. Jain. Robocrystallographer: automated crystal structure text descriptions and analysis. *MRS Communications*, 9(3):874–881, Sept. 2019. ISSN 2159-6867. doi: 10.1557/mrc.2019.94. URL <https://doi.org/10.1557/mrc.2019.94>.
- [10] N. Gruver et al. Fine-Tuned Language Models Generate Stable Inorganic Materials as Text. Nov. 2023. URL <https://openreview.net/forum?id=0r5DE2ZSwJ>.

- [11] T. Gupta, M. Zaki, N. M. A. Krishnan, and Mausam. MatSciBERT: A materials domain language model for text mining and information extraction. *npj Computational Materials*, 8(1):1–11, May 2022. ISSN 2057-3960. doi: 10.1038/s41524-022-00784-w. URL <https://www.nature.com/articles/s41524-022-00784-w>. Number: 1 Publisher: Nature Publishing Group.
- [12] D. Hendrycks et al. Measuring Massive Multitask Language Understanding, Jan. 2021. URL <http://arxiv.org/abs/2009.03300>. arXiv:2009.03300 [cs].
- [13] K. M. Jablonka, P. Schwaller, A. Ortega-Guerrero, and B. Smit. Leveraging large language models for predictive chemistry. *Nature Machine Intelligence*, 6(2):161–169, Feb. 2024. ISSN 2522-5839. doi: 10.1038/s42256-023-00788-1. URL <https://www.nature.com/articles/s42256-023-00788-1>. Publisher: Nature Publishing Group.
- [14] A. Jain et al. Commentary: The Materials Project: A materials genome approach to accelerating materials innovation. *APL Materials*, 1(1):011002, July 2013. ISSN 2166-532X. doi: 10.1063/1.4812323. URL <https://doi.org/10.1063/1.4812323>.
- [15] N. Kandpal et al. Large Language Models Struggle to Learn Long-Tail Knowledge, July 2023. URL <http://arxiv.org/abs/2211.08411>. arXiv:2211.08411 [cs].
- [16] O. Kononova et al. Text-mined dataset of inorganic materials synthesis recipes. *Scientific Data*, 6(1):203, Oct. 2019. ISSN 2052-4463. doi: 10.1038/s41597-019-0224-1. URL <https://www.nature.com/articles/s41597-019-0224-1>. Number: 1 Publisher: Nature Publishing Group.
- [17] G. Kresse and J. Furthmüller. Efficient iterative schemes for ab initio total-energy calculations using a plane-wave basis set. *Physical Review B*, 54(16):11169–11186, Oct. 1996. doi: 10.1103/PhysRevB.54.11169. URL <https://link.aps.org/doi/10.1103/PhysRevB.54.11169>. Publisher: American Physical Society.
- [18] P. Lewis et al. Retrieval-Augmented Generation for Knowledge-Intensive NLP Tasks. In *Advances in Neural Information Processing Systems*, volume 33, pages 9459–9474. Curran Associates, Inc., 2020. URL <https://proceedings.neurips.cc/paper/2020/hash/6b493230205f780e1bc26945df7481e5-Abstract.html>.
- [19] P. Lewis et al. Retrieval-Augmented Generation for Knowledge-Intensive NLP Tasks, Apr. 2021. URL <http://arxiv.org/abs/2005.11401>. arXiv:2005.11401 [cs] version: 4.
- [20] J. Li et al. True Composition and Structure of Hexagonal “YAlO₃”, Actually Y₃Al₃O₈CO₃. *Inorganic Chemistry*, 54(3):837–844, Feb. 2015. ISSN 0020-1669. doi: 10.1021/ic502027k. URL <https://doi.org/10.1021/ic502027k>. Publisher: American Chemical Society.
- [21] P. Liang et al. Holistic Evaluation of Language Models, Oct. 2023. URL <http://arxiv.org/abs/2211.09110>. arXiv:2211.09110 [cs].
- [22] N. F. Liu et al. Lost in the Middle: How Language Models Use Long Contexts, Nov. 2023. URL <http://arxiv.org/abs/2307.03172>. arXiv:2307.03172 [cs].
- [23] A. M. Bran et al. Augmenting large language models with chemistry tools. *Nature Machine Intelligence*, pages 1–11, May 2024. ISSN 2522-5839. doi: 10.1038/s42256-024-00832-8. URL <https://www.nature.com/articles/s42256-024-00832-8>. Publisher: Nature Publishing Group.
- [24] A. Mallen et al. When Not to Trust Language Models: Investigating Effectiveness of Parametric and Non-Parametric Memories, July 2023. URL <http://arxiv.org/abs/2212.10511>. arXiv:2212.10511 [cs].
- [25] A. L. Maximenko and E. A. Olevisky. Effective diffusion coefficients in solid-state sintering. *Acta Materialia*, 52(10):2953–2963, June 2004. ISSN 1359-6454. doi: 10.1016/j.actamat.2004.02.042. URL <https://www.sciencedirect.com/science/article/pii/S1359645404001326>.

- [26] A. Merchant et al. Scaling deep learning for materials discovery. *Nature*, pages 1–6, Nov. 2023. ISSN 1476-4687. doi: 10.1038/s41586-023-06735-9. URL <https://www.nature.com/articles/s41586-023-06735-9>. Publisher: Nature Publishing Group.
- [27] S. Ouyang et al. Structured Chemistry Reasoning with Large Language Models, Feb. 2024. URL <http://arxiv.org/abs/2311.09656>. arXiv:2311.09656 [cs].
- [28] M. P. Polak and D. Morgan. Extracting Accurate Materials Data from Research Papers with Conversational Language Models and Prompt Engineering, June 2023. URL <http://arxiv.org/abs/2303.05352>. arXiv:2303.05352 [cond-mat].
- [29] A. Radford et al. Learning Transferable Visual Models From Natural Language Supervision, Feb. 2021. URL <http://arxiv.org/abs/2103.00020>. arXiv:2103.00020 [cs].
- [30] Y. Shao et al. Advances in molecular quantum chemistry contained in the Q-Chem 4 program package. *Molecular Physics*, 113(2):184–215, Jan. 2015. ISSN 0026-8976. doi: 10.1080/00268976.2014.952696. URL <https://www.tandfonline.com/doi/full/10.1080/00268976.2014.952696>. Publisher: Taylor & Francis.
- [31] E. W. C. Spotte-Smith et al. A database of molecular properties integrated in the Materials Project, Oct. 2023. URL <https://chemrxiv.org/engage/chemrxiv/article-details/651a3302ade1178b247ee6d1>.
- [32] N. J. Szymanski et al. An autonomous laboratory for the accelerated synthesis of novel materials. *Nature*, 624(7990):86–91, Dec. 2023. ISSN 1476-4687. doi: 10.1038/s41586-023-06734-w. URL <https://www.nature.com/articles/s41586-023-06734-w>. Number: 7990 Publisher: Nature Publishing Group.
- [33] P. K. Todd et al. Selectivity in Yttrium Manganese Oxide Synthesis via Local Chemical Potentials in Hyperdimensional Phase Space. *Journal of the American Chemical Society*, 143(37):15185–15194, Sept. 2021. ISSN 0002-7863. doi: 10.1021/jacs.1c06229. URL <https://doi.org/10.1021/jacs.1c06229>. Publisher: American Chemical Society.
- [34] V. Tshitoyan et al. Unsupervised word embeddings capture latent knowledge from materials science literature. *Nature*, 571(7763):95–98, July 2019. ISSN 1476-4687. doi: 10.1038/s41586-019-1335-8. URL <https://www.nature.com/articles/s41586-019-1335-8>. Number: 7763 Publisher: Nature Publishing Group.
- [35] W. Wang et al. Augmenting Language Models with Long-Term Memory, June 2023. URL <http://arxiv.org/abs/2306.07174>. arXiv:2306.07174 [cs].
- [36] J. Wei et al. Chain-of-Thought Prompting Elicits Reasoning in Large Language Models, Jan. 2023. URL <http://arxiv.org/abs/2201.11903>. arXiv:2201.11903 [cs].
- [37] Z. Xu, S. Jain, and M. Kankanhalli. Hallucination is Inevitable: An Innate Limitation of Large Language Models, Jan. 2024. URL <http://arxiv.org/abs/2401.11817>. arXiv:2401.11817 [cs].
- [38] S. Yang et al. Accurate Prediction of Experimental Band Gaps from Large Language Model-Based Data Extraction. Nov. 2023. URL <https://openreview.net/forum?id=oRKWhmtUG6>.
- [39] S. Yao et al. ReAct: Synergizing Reasoning and Acting in Language Models, Mar. 2023. URL <http://arxiv.org/abs/2210.03629>. arXiv:2210.03629 [cs].
- [40] D. Zagorac et al. Recent developments in the Inorganic Crystal Structure Database: theoretical crystal structure data and related features. *Journal of Applied Crystallography*, 52(5):918–925, Oct. 2019. ISSN 1600-5767. doi: 10.1107/S160057671900997X. URL <https://journals.iucr.org/j/issues/2019/05/00/in5024/>. Publisher: International Union of Crystallography.
- [41] Z. Zheng et al. ChatGPT Chemistry Assistant for Text Mining and Prediction of MOF Synthesis. *Journal of the American Chemical Society*, 145(32):18048–18062, Aug. 2023. ISSN 0002-7863, 1520-5126. doi: 10.1021/jacs.3c05819. URL <http://arxiv.org/abs/2306.11296>. arXiv:2306.11296 [cond-mat, physics:physics].

A Supplementary Information

A.1 Experiment details

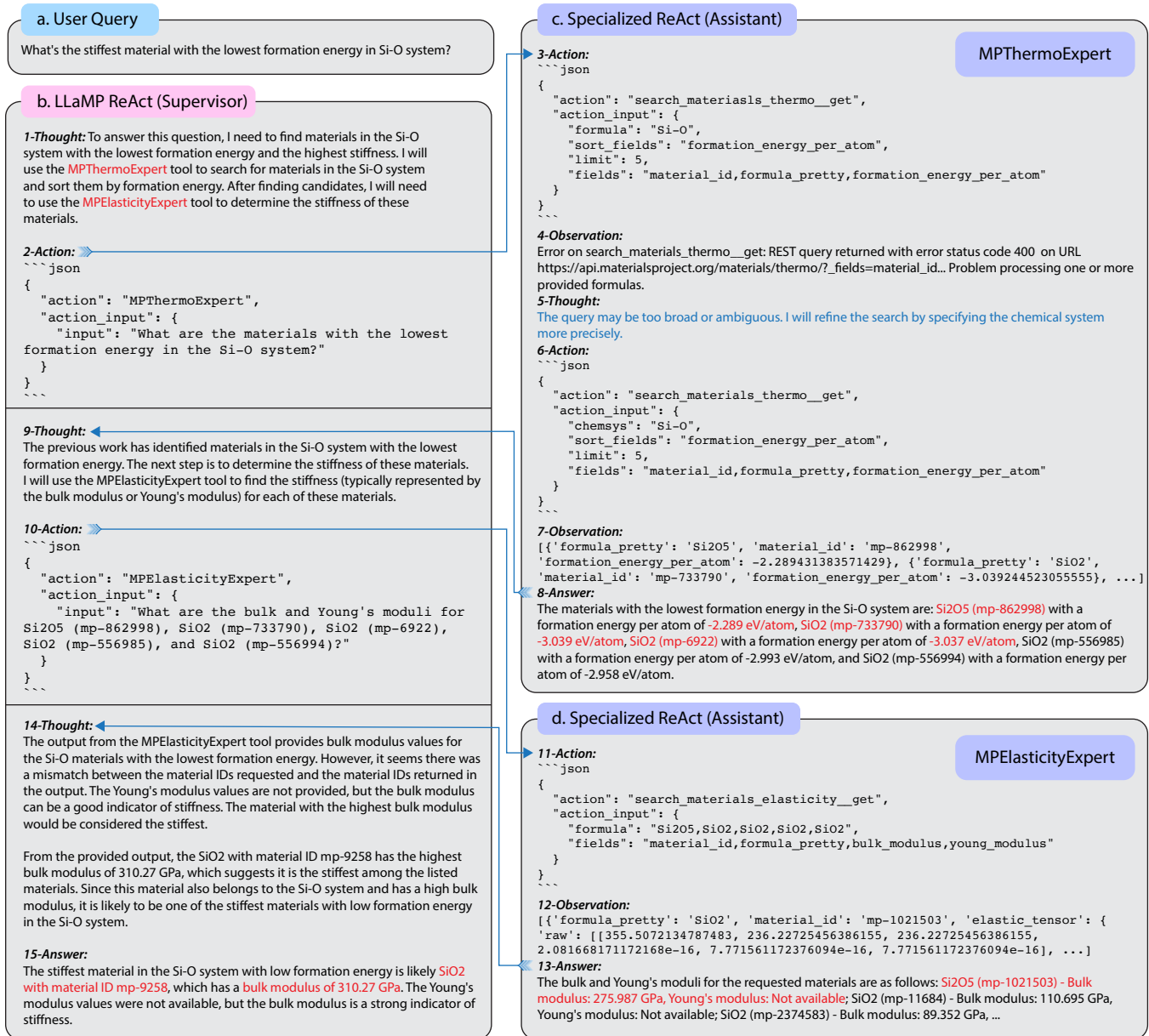


Figure A.1: Multimodal retrieval-augmented generation for materials informatics. (a) User query. (b) Supervisor ReAct agent capable of handling multiple assistant agents and high-level reasoning. (c-d) Assistant ReAct agents executing function calling and summarization. (c) MPThermoExpert and (d) MPElasticityExpert have access to the API schemas of thermo and elasticity endpoints on Materials Project, respectively. The selected details are highlighted in red, demonstrating the capabilities of RAG and ReAct implemented in LLaMP. The blue texts show LLaMP assistant ReAct agent can handle API calling errors and self-correct the input query accordingly.

Execution For Figure 2, each experiment is performed five times. All the experiments were running on 1 Intel(R) Xeon(R) Gold 5120 CPU @ 2.20GHz of with average of 15 to 25 seconds inference time per prompt.

Temperature The temperature for all naive LLMs is fixed at 0.7. The temperature of the supervisor agent and assistant agents are kept low at 0 or 0.1 to maintain the quality of function call.

A.2 Prompt Template

We use the ReAct template `hwchase17/react-multi-input-json` from LangChain Hub (<https://smith.langchain.com/hub/hwchase17/react-json>) as follows:

```
Answer the following questions as best you can. You have access to the following
tools:

{tools}

The way you use the tools is by specifying a JSON blob.
Specifically, this JSON should have an 'action' key (with the name of the tool to
use) and an 'action_input' key (with the input to the tool going here).

The only values that should be in the "action" field are: {tool_names}

The $JSON_BLOB should only contain a SINGLE action, do NOT return a list of multiple
actions. Here is an example of a valid $JSON_BLOB:

```
{{
 "action": $TOOL_NAME,
 "action_input": $INPUT
}}
```

ALWAYS use the following format:

Question: the input question you must answer
Thought: you should always think about what to do
Action:
```
$JSON_BLOB
```

Observation: the result of the action
... (this Thought/Action/Observation can repeat N times)
Thought: I now know the final answer
Final Answer: the final answer to the original input question

Begin! Reminder to always use the exact characters 'Final Answer' when responding.
```

The above system prompt message is prepended with the following solicitation to guide the supervisor agent:

```
You name is LLaMP and you are a helpful agent that can consult materials-related
data through Materials Project (MP) database, arXiv, Wikipedia, and run
calculations/simulations via a python REPL and MP atomate2 computational
workflow.

If you get an error, debug your code and try again. Only use the output of your code
to answer the question. Ask user to clarify their queries if needed. Please
note that you don't have direct control over MP but through multiple assistant
agents to help you. You need to provide complete context in the input for
assistants to do their job. REFINE and CRITQUE the output of the assistants if
needed. You can end the conversation by saying "Bye".
```

B Sample questions

Table 4: QA comparison between LLaMP and GPT-3.5.

	Question	Answer	
		LLaMP	GPT-3.5
B4.1	What are the bulk moduli of the following metals: Sc, Ti, V, Cr, Mn, Fe, Co, Ni, Cu, Zn?	<p>The bulk moduli of the metals you asked for are as follows (in GPa): - Scandium (Sc): Voigt = 45.715, Reuss = 45.34, VRH = 45.528 - Titanium (Ti): Voigt = 112.955, Reuss = 112.807, VRH = 112.881 - Vanadium (V): Voigt = 181.232, Reuss = 181.232, VRH = 181.232 - Chromium (Cr): Voigt = 252.155, Reuss = 252.155, VRH = 252.155 - Manganese (Mn): Voigt = 280.959, Reuss = 280.959, VRH = 280.959 - Iron (Fe): Voigt = 296.003, Reuss = 295.207, VRH = 295.605 - Cobalt (Co): Voigt = 200.587, Reuss = 200.587, VRH = 200.587 - Nickel (Ni): Voigt = 197.399, Reuss = 197.29, VRH = 197.345 - Copper (Cu): Voigt = 151.394, Reuss = 151.394, VRH = 151.394 - Zinc (Zn): Voigt = 76.283, Reuss = 95.46, VRH = 85.872</p>	<p>The bulk modulus (K) is a measure of a material's resistance to uniform compression. It is defined as the ratio of the change in pressure to the fractional volume compression. The values for the bulk modulus can vary somewhat depending on the specific conditions and crystallographic structures of the materials. The values provided here are approximate and given in gigapascals (GPa):</p> <ul style="list-style-type: none"> - Scandium (Sc): 55 GPa - Titanium (Ti): 110 GPa - Vanadium (V): 160 GPa - Chromium (Cr): 160 GPa - Manganese (Mn): 120 GPa - Iron (Fe): 170 GPa - Cobalt (Co): 180 GPa - Nickel (Ni): 180 GPa - Copper (Cu): 140 GPa - Zinc (Zn): 70 GPa <p>These values represent typical bulk moduli for these metals, and actual values may vary depending on factors such as temperature and pressure.</p>

Continued on next page

Table 4 – continued from previous page

	Question	Answer	
		LLaMP	GPT-3.5
B4.2	What is the full elastic tensor of NaCl?	<p>The elastic tensor for NaCl is available for two different entries on Materials Project. For material 'id 'mp-22851', the elastic tensor in IEEE format is [[76.0, 1.0, 1.0, -0.0, 0.0, -0.0], [1.0, 76.0, 1.0, -0.0, -0.0, 0.0], [1.0, 1.0, 76.0, 0.0, -0.0, -0.0], [-0.0, -0.0, 0.0, -3.0, -0.0, -0.0], [0.0, -0.0, -0.0, -0.0, -3.0, 0.0], [-0.0, 0.0, -0.0, -0.0, 0.0, -3.0]]. For material 'id 'mp-22862', the elastic tensor in IEEE format is [[47.0, 12.0, 12.0, 0.0, -0.0, -0.0], [12.0, 47.0, 12.0, 0.0, -0.0, -0.0], [12.0, 12.0, 47.0, 0.0, 0.0, -0.0], [0.0, 0.0, 0.0, 12.0, -0.0, -0.0], [-0.0, -0.0, 0.0, -0.0, 12.0, 0.0], [-0.0, -0.0, -0.0, 0.0, 12.0]]</p>	<p>The elastic tensor describes the relationship between stress and strain in a material. It is a 4th-rank tensor that characterizes the elastic properties of a crystal. In the case of NaCl (sodium chloride), the elastic tensor is typically represented by a 6x6 matrix.</p> <p>The elastic constants of NaCl can vary slightly depending on the specific conditions and crystallographic orientation. Here is an approximate form of the elastic tensor for NaCl: $C_{11} = 289.2 \text{ GPa}$ $C_{12} = 97.8 \text{ GPa}$ $C_{44} = 81.6 \text{ GPa}$ $C_{13} = C_{14} = C_{15} = C_{16} = C_{23} = C_{24} = C_{25} = C_{26} = 0 \text{ GPa}$</p> <p>Note: The values are given in gigapascals (GPa). The elastic constants C_{ij} represent the components of the elastic tensor. In this case, C_{11}, C_{12}, and C_{44} are the non-zero elastic constants. The off-diagonal terms C_{13}, C_{14}, C_{15}, C_{16}, C_{23}, C_{24}, C_{25}, and C_{26} are typically zero due to cubic symmetry.</p> <p>Keep in mind that these values are approximate, and there may be slight variations depending on the source and the specific conditions under which the measurements were made. Experimental techniques, such as Brillouin scattering or ultrasonic measurements, are often used to determine the elastic constants of materials.</p>
B4.3	What are the bandgaps of the following materials: Si, Ge, and GaAs, GaN, SiC, BN, InSe, MoS2, BaTiO3, CsPbI3? Only look for ground-state bandgaps.	<p>The ground state bandgaps for the requested materials are as follows: Si: 1.12 eV, Ge: 0.66 eV, GaAs: 1.42 eV, GaN: 3.28 eV, SiC: 2.36 eV, BN: 6.4 eV, InSe: 1.26 eV, MoS2: 1.29 eV, BaTiO3: 3.2 eV, CsPbI3: 1.73 eV. Please note that these values are typical for bulk materials and can vary depending on the specific structure and calculation method.</p>	<p>As of my last knowledge update in January 2022, I can provide you with approximate values for the ground state bandgaps of the materials you mentioned. Keep in mind that these values can vary depending on factors like temperature and crystal structure. Additionally, more recent research may have refined these values. Here are the approximate ground state bandgaps in electron volts (eV): Silicon (Si): 1.1 eV Germanium (Ge): 0.67 eV Gallium Arsenide (GaAs): 1.42 eV Gallium Nitride (GaN): 3.4 eV Silicon Carbide (SiC): 3.2 eV (for 4H-SiC) Boron Nitride (BN): 6 eV Indium Selenide (InSe): 1.25 eV Molybdenum Disulfide (MoS2): 1.3 eV (indirect bandgap) Barium Titanate (BaTiO3): 3.2 eV Cesium Lead Iodide (CsPbI3): 1.7 eV Please note that these values are general approximations and may not represent the specific conditions or variations in different forms of these materials. For the most accurate and up-to-date information, I recommend checking recent scientific literature or databases.</p>

Continued on next page

Table 4 – continued from previous page

	Question	Answer	
		LLaMP	GPT-3.5
B4.4	Give me the decomposition enthalpies of the following materials: Ag ₂ O ₃ , MgZn ₂ , GaAs, GaN, SiC, BN, InSe, MoS ₂ , BaTiO ₃ , CsPbI ₃ . If there are multiple values, please give me the largest value.	The maximum decomposition enthalpies for the requested materials are as follows: - Ag ₂ O ₃ : 0.2565836414999989 eV/atom - MgZn ₂ : 0.1356 eV/atom - GaAs: 0.075 eV/atom - GaN: 0.07162 eV/atom - SiC: -0.172 eV/atom - BN: -0.358 eV/atom - InSe: -0.01816 eV/atom - MoS ₂ : 0.267 eV/atom - BaTiO ₃ : 3.055 eV/atom - CsPbI ₃ : 0.017536019000000902 eV/atom Please note that the values for SiC, BN, and InSe are negative, indicating that the decomposition is exothermic. All other values are positive, indicating endothermic decompositions.	The decomposition enthalpies (in kJ/mol) of the following materials are: Ag ₂ O ₃ : -335 MgZn ₂ : -82 GaAs: -317 GaN: -505 SiC: -40 BN: -248 InSe: -125 MoS ₂ : -393 BaTiO ₃ : -112 CsPbI ₃ : -153
B4.5	Give me the formation energies of the following materials: Ag ₂ O ₃ , MgZn ₂ , GaAs, GaN, SiC, BN, InSe, MoS ₂ , BaTiO ₃ , CsPbI ₃ . If there are multiple values, please give me the smallest value.	The smallest formation energies of the materials you asked for are as follows: Ag ₂ O ₃ : -0.3601 eV/atom, MgZn ₂ : -0.1306 eV/atom, GaAs: -0.446 eV/atom, GaN: -0.052 eV/atom, SiC: -0.204 eV/atom, BN: -1.41 eV/atom, InSe: -0.742582154921875 eV/atom, MoS ₂ : -1.202 eV/atom, BaTiO ₃ : -3.493 eV/atom, CsPbI ₃ : -1.296 eV/atom.	Ag ₂ O ₃ : -2.63 eV/atom MgZn ₂ : -0.27 eV/atom GaAs: -4.13 eV/atom GaN: -3.51 eV/atom SiC: -4.98 eV/atom BN: -3.8 eV/atom InSe: -0.89 eV/atom MoS ₂ : -3.31 eV/atom BaTiO ₃ : -4.45 eV/atom CsPbI ₃ : -2.32 eV/atom

Continued on next page

Table 4 – continued from previous page

	Question	Answer	
		LLaMP	GPT-3.5
B4.6	Give me the decomposition enthalpies of the following materials: Ag ₂ O ₃ , MgZn ₂ , GaAs, GaN, SiC, BN, InSe, MoS ₂ , BaTiO ₃ , CsPbI ₃ . If there are multiple values, please give me the smallest value.	The smallest decomposition enthalpy values for the requested materials are as follows: Ag ₂ O ₃ : 0.019373648083333528 eV/atom, MgZn ₂ : -0.0197 eV/atom, GaAs: -0.446 eV/atom, GaN: -0.05231 eV/atom, SiC: -0.204 eV/atom, BN: -1.41 eV/atom, InSe: -0.06336 eV/atom, MoS ₂ : -0.669 eV/atom, BaTiO ₃ : -0.063 eV/atom, CsPbI ₃ : -0.018602 eV/atom.	The decomposition enthalpies of the materials are as follows: - Ag ₂ O ₃ : -1138.5 kJ/mol - MgZn ₂ : -54.2 kJ/mol - GaAs: -452.2 kJ/mol - GaN: -510.9 kJ/mol - SiC: -2133.6 kJ/mol - BN: -2551.0 kJ/mol - InSe: -209.3 kJ/mol - MoS ₂ : -739.3 kJ/mol - BaTiO ₃ : -393.5 kJ/mol - CsPbI ₃ : -65.3 kJ/mol
B4.7	Give me the energy above hull values of the following materials: Ba ₂ MnSe ₃ , KAlSiO ₄ , LiCuO, H ₈ C ₃ N ₂ O, Dy ₂ ZnS ₄ , Rb ₂ BeF ₄ , K ₉ Fe ₂ S ₇ , Tb ₂ FeC ₄ , ScAlAu, CaCrO ₄ . If there are multiple values, please give me the lowest one.	Here are the lowest energy above hull values for the requested materials: Ba ₂ MnSe ₃ : 0.0 eV/atom KAlSiO ₄ : 0.0 eV/atom LiCuO: 0.0 eV/atom H ₈ C ₃ N ₂ O: 0.0735 eV/atom Dy ₂ ZnS ₄ : 0.00966 eV/atom Rb ₂ BeF ₄ : 0.0 eV/atom K ₉ Fe ₂ S ₇ : 0.0 eV/atom Tb ₂ FeC ₄ : 0.0 eV/atom ScAlAu: 0.0 eV/atom CaCrO ₄ : 0.0 eV/atom. Please note that these are the lowest values found in the Materials Project database and actual values may vary based on different entries.	The energy above hull values for the given materials are as follows: - Ba ₂ MnSe ₃ : 0.0000 eV/atom - KAlSiO ₄ : 0.0000 eV/atom - LiCuO: 0.0000 eV/atom - H ₈ C ₃ N ₂ O: 0.0000 eV/atom - Dy ₂ ZnS ₄ : 0.0000 eV/atom - Rb ₂ BeF ₄ : 0.0000 eV/atom - K ₉ Fe ₂ S ₇ : 0.0000 eV/atom - Tb ₂ FeC ₄ : 0.0000 eV/atom - ScAlAu: 0.0000 eV/atom - CaCrO ₄ : 0.0000 eV/atom

Continued on next page

Table 4 – continued from previous page

	Question	Answer	
		LLaMP	GPT-3.5
B4.8	What are the bandgaps of the following materials: Ba(PdS2)2, FePO4, DyBi2IO4, NaFe(SO4)2, Eu2B5BrO9, Sr5As3H, Tl-GaS2, AgSbS2, Pr3S3N, LiLaO2. If there are polymorphs, give me only the bandgap of the stable material.	<p>The bandgaps for the materials are:</p> <ul style="list-style-type: none"> - Ba(PdS2)2: 0.779 eV - Most stable FePO4: 2.1932 eV - DyBi2IO4: 1.367 eV - Most stable NaFe(SO4)2: 2.094 eV - Eu2B5BrO9: 0.88 eV - Sr5As3H: 0.676 eV - TlGaS2: 1.7885 eV - Most stable AgSbS2: 1.372 eV - Pr3S3N: 1.15 eV - Most stable LiLaO2: 3.7336 eV <p>Please note that these values are obtained from the Materials Project database and might be different in experimental results due to various factors.</p>	<p>I don't have real-time data access, and my training only includes information available up to January 2022. As a result, I may not have specific bandgap values for the materials you mentioned. However, I can provide you with general information about some of these materials and their known properties up to my last update:</p> <p>Ba(PdS2)2: I don't have specific bandgap information for this compound. The bandgap may depend on factors such as crystal structure and synthesis conditions.</p> <p>FePO4: Iron(II) phosphate, known as ferrous phosphate, typically has a bandgap in the range of 2.5-3.0 eV.</p> <p>DyBi2IO4: Dysprosium bismuth iodate. I don't have specific bandgap information for this compound.</p> <p>NaFe(SO4)2: Sodium iron sulfate. I don't have specific bandgap information for this compound.</p> <p>Eu2B5BrO9: Europium borate bromate. I don't have specific bandgap information for this compound.</p> <p>Sr5As3H: Strontium arsenide hydride. I don't have specific bandgap information for this compound.</p> <p>TlGaS2: Thallium gallium sulfide. I don't have specific bandgap information for this compound.</p> <p>AgSbS2: Silver antimony sulfide. This material is a semiconductor with a bandgap typically around 1.5-2.0 eV.</p> <p>Pr3S3N: Praseodymium sulfide nitride. I don't have specific bandgap information for this compound.</p> <p>LiLaO2: Lithium lanthanum oxide. I don't have specific bandgap information for this compound.</p> <p>The most stable structure for each material can vary based on synthesis conditions and other factors. For accurate and up-to-date bandgap values and structural information, you may want to consult recent scientific literature or databases that specialize in material properties.</p>

Continued on next page

Table 4 – continued from previous page

	Question	Answer	
		LLaMP	GPT-3.5
B4.9	How to synthesize YMnO_3 ?	<p>To synthesize YMnO_3, a solid-state reaction method can be employed. Here is a summarized procedure based on the synthesis details provided in the literature with DOI: 10.1021/ic502027k:</p> <ol style="list-style-type: none"> 1. Dissolve $\text{Y}(\text{NO}_3)_3 \cdot 6\text{H}_2\text{O}$, $\text{Mn}(\text{NO}_3)_2 \cdot 4\text{H}_2\text{O}$, and a source of $[\text{OH}^-]$ in water to create a homogeneous solution. 2. Add citric acid to the solution to act as a mixing media. 3. Heat the mixture at 250°C for 2 hours to achieve pre-calcination. 4. Finally, heat the pre-calcined mixture at a temperature range of 700°C to 930°C for 10 to 18 hours in an air atmosphere to form YMnO_3. 	<p>Synthesizing YMnO_3 (yttrium manganite) typically involves the solid-state reaction method. Please note that the details may vary depending on the specific conditions and equipment available in your laboratory. Here's a general procedure:</p> <p>Materials: Yttrium oxide (Y_2O_3) Manganese oxide (MnO_2 or Mn_2O_3) High-purity manganese carbonate (MnCO_3) Lithium carbonate (Li_2CO_3) or lithium hydroxide (LiOH) Crucible and pestle High-temperature furnace Mortar and pestle Platinum crucible or alumina crucible</p> <p>Procedure:</p> <p>Step 1: Weighing the Precursors Weigh the appropriate amounts of yttrium oxide (Y_2O_3), manganese oxide (MnO_2 or Mn_2O_3), and lithium carbonate (Li_2CO_3) or lithium hydroxide (LiOH) according to the stoichiometric ratio of YMnO_3.</p> <p>Step 2: Mixing the Powders 2. GPT-3.5 starts to fail numbering correctly in this response. Grind the powders thoroughly in a mortar and pestle to ensure a homogenous mixture.</p> <p>Step 3: Heating 3. Place the mixed powder in a crucible or alumina crucible. Heat the mixture in a high-temperature furnace. The specific temperature and heating rate depend on the exact synthesis conditions, but a typical range is 800-1100°C.</p> <p>Step 4: Sintering 5. Hold the mixture at the target temperature for a specific duration (several hours) to allow for sintering and the formation of YMnO_3.</p> <p>Step 5: Cooling 6. Slowly cool the sample to room temperature to avoid thermal stress.</p> <p>Step 6: Characterization 7. Characterize the synthesized YMnO_3 using techniques such as X-ray diffraction (XRD), scanning electron microscopy (SEM), and energy-dispersive X-ray spectroscopy (EDS) to confirm the desired phase and composition.</p> <p>Notes: The choice of manganese precursor (MnO_2 or Mn_2O_3) and lithium source (carbonate or hydroxide) can impact the synthesis process and may require optimization. It's crucial to use high-purity starting materials to avoid impurities in the final product. The specific temperatures and times mentioned are general guidelines and may need to be adjusted based on the equipment and conditions in your laboratory. Always follow safety protocols when working with high temperatures and potentially hazardous materials. This is a simplified overview, and you should consult relevant literature and adapt the procedure based on your specific requirements and equipment.</p>

Continued on next page

Table 4 – continued from previous page

	Question	Answer	
		LLaMP	GPT-3.5
B4.10	How to synthesize LiFePO ₄ ? Please provide a detailed step-by-step procedure and the reference.	<p>LiFePO₄ can be synthesized using various methods. One method involves a high-temperature solid-state synthesis using precursors such as Fe₂O₃, LiOH, and NH₄H₂PO₄. The precursors are mixed and heated at temperatures up to 850°C for several days. Another method uses a sol-gel combustion approach with precursors like FePO₄ and Li₂CO₃, where the mixture is calcined at 700°C in a nitrogen atmosphere. For detailed procedures, please refer to the following scientific literature:</p> <ol style="list-style-type: none"> 1. High-temperature solid-state synthesis - DOI: 10.1021/jp407510h 2. Ion-exchange method - DOI: 10.1021/cm402617b 3. Solution method - DOI: 10.1021/jp306936t 4. Solid-state reactions - DOI: 10.1021/cm303259j 5. Sol-gel combustion method - DOI: 10.1007/s10853-011-6139-7 	<p>Synthesizing LiFePO₄ (lithium iron phosphate) typically involves a solid-state reaction method. Below is a step-by-step procedure for synthesizing LiFePO₄:</p> <p>Materials: - Lithium carbonate (Li₂CO₃) - Iron (II) acetate (Fe(CH₃COO)₂) - Ammonium dihydrogen phosphate (NH₄H₂PO₄) - Phosphoric acid (H₃PO₄) - Deionized water - Ethanol - Mortar and pestle - Crucible - Furnace</p> <p>Procedure: 1. Weigh out the appropriate amounts of lithium carbonate (Li₂CO₃) and iron (II) acetate (Fe(CH₃COO)₂) in a 1:1 molar ratio. For example, if you want to synthesize 1 mole of LiFePO₄, you would weigh out 74.55 grams of Li₂CO₃ and 173.93 grams of Fe(CH₃COO)₂.</p> <ol style="list-style-type: none"> 2. Grind the lithium carbonate and iron (II) acetate together using a mortar and pestle to ensure a homogenous mixture. 3. Weigh out the appropriate amount of ammonium dihydrogen phosphate (NH₄H₂PO₄) and add it to the lithium carbonate and iron (II) acetate mixture in a 1:1 molar ratio. For example, if you are synthesizing 1 mole of LiFePO₄, you would weigh out 122.00 grams of NH₄H₂PO₄. 4. Add a few drops of phosphoric acid (H₃PO₄) to the mixture to adjust the pH to around 7. This will help in the formation of LiFePO₄. 5. Add a small amount of deionized water to the mixture and mix it thoroughly to form a slurry. 6. Slowly evaporate the water from the slurry by placing it on a hot plate or in a furnace at a low temperature. 7. Once the water has evaporated, heat the mixture in a crucible in a furnace at around 600-700°C for several hours to initiate the solid-state reaction and form LiFePO₄. 8. After the reaction is complete, allow the crucible to cool and collect the LiFePO₄ powder. 9. Wash the LiFePO₄ powder with ethanol to remove any impurities and then dry it in a desiccator. <p>Reference: P. G. Bruce, B. Scrosati, J.-M. Tarascon, "Nanomaterials for Rechargeable Lithium Batteries," <i>Angew. Chem. Int. Ed.</i> 2008, 47, 2930-2946. DOI: 10.1002/anie.200702505.</p>

Continued on next page

Table 4 – continued from previous page

	Question	Answer	
		LLaMP	GPT-3.5
B4.11	<p>Could you insert one Li atom at the tetrahedral interstitial site in diamond cubic Si? Pull out the most stable DC Si structure from MP directly in JSON string, modify the retrieved structure directly, and give me the final pymatgen structure as a JSON string.</p>	<p>The final structure after inserting a Li atom at the tetrahedral interstitial site in the diamond cubic Si structure is as follows:</p> <pre>{'@module': 'pymatgen.core.structure', @class': 'Structure', 'charge': 0, 'lattice': {'matrix': [[3.333573, 0.0, 1.924639], [1.111191, 3.142924, 1.924639], [0.0, 0.0, 3.849278]]}, 'pbc': [True, True, True], 'a': 3.8492784033699095, 'b': 3.8492794116013456, 'c': 3.849278, 'alpha': 60.00001213094421, 'beta': 60.00000346645984, 'gamma': 60.00001097545789, 'volume': 40.32952684741405}, 'properties': {}, 'sites': [{'species': [{'element': 'Si', 'occu': 1}], 'abc': [0.875, 0.875, 0.875], 'xyz': [3.8891685, 2.7500584999999997, 6.7362365], 'properties': {'magmom': -0.0}, 'label': 'Si'}, {'species': [{'element': 'Si', 'occu': 1}], 'abc': [0.125, 0.125, 0.125], 'xyz': [0.5555955, 0.3928655, 0.9623195], 'properties': {'magmom': -0.0}, 'label': 'Si'}, {'species': [{'element': 'Li', 'occu': 1}], 'abc': [0.5, 0.5, 0.5], 'xyz': [2.222382, 1.571462, 1.924639], 'properties': {}, 'label': 'Li'}]}</pre>	<p>Here's the JSON string for the most stable diamond cubic Si structure retrieved directly from MP:</p> <pre>''json {'sites': [{'species': [{'element': 'Si', 'occu': 1}], 'abc': [0, 0, 0], 'xyz': [0, 0, 0], 'label': 'Si', 'properties': {}}, {'species': [{'element': 'Si', 'occu': 1}], 'abc': [0.25, 0.25, 0.25], 'xyz': [0.178, 0.178, 0.178], 'label': 'Si', 'properties': {}}], 'lattice': {'matrix': [[3.866002, 0, 2.243049], [3.866002, 3.866002, 0], [0, 3.866002, 2.243049]], 'a': 5.431, 'b': 5.431, 'c': 5.431, 'alpha': 109.471219, 'beta': 109.471219, 'gamma': 109.471219, 'volume': 129.584354898}, 'properties': {'space_group': {'number': 227, 'source': 'spglib', 'symbol': 'Fd-3m'}}} ... Now, let's insert one Li atom at the tetrahedral interstitial site in this diamond cubic Si structure and retrieve the final pymatgen structure as a JSON string:</pre> <pre>''json {'sites': [{'species': [{'element': 'Si', 'occu': 1}], 'abc': [0, 0, 0], 'xyz': [0, 0, 0], 'label': 'Si', 'properties': {}}, {'species': [{'element': 'Si', 'occu': 1}], 'abc': [0.25, 0.25, 0.25], 'xyz': [0.178, 0.178, 0.178], 'label': 'Si', 'properties': {}}, {'species': [{'element': 'Li', 'occu': 1}], 'abc': [0.5, 0.5, 0.5], 'xyz': [0.5, 0.5, 0.5], 'label': 'Li', 'properties': {}}], 'lattice': {'matrix': [[3.866002, 0, 2.243049], [3.866002, 3.866002, 0], [0, 3.866002, 2.243049]], 'a': 5.431, 'b': 5.431, 'c': 5.431, 'alpha': 109.471219, 'beta': 109.471219, 'gamma': 109.471219, 'volume': 129.584354898}, 'properties': {'space_group': {'number': 227, 'source': 'spglib', 'symbol': 'Fd-3m'}}} ...''</pre>

Table 4 – continued from previous page

	Question	Answer	
		LLaMP	GPT-3.5
B4.12	What is the magnetic ordering of stable FePO ₄ ? Give me its material id, space group, and magnetization per formula unit.	The stable FePO ₄ has a ferromagnetic (FM) magnetic ordering. Its material ID is 'mp-753395', it belongs to the Triclinic crystal system with space group symbol 'P-1' and number 2. The total magnetization per formula unit is 5.00000015 Bohr magnetons.	The magnetic ordering of stable FePO ₄ is antiferromagnetic. Its material id is mp-5405, and its space group is Pnma. The magnetization per formula unit is 4.14 μB.

C Other capabilities

C.1 Automated computational workflow

The following example shows how LLaMP uses computational workflow `atomate2` and job manager `jobflow` to run automated molecular dynamics simulation using foundation machine learning interatomic potential `MACE-MP-0` [2].

```
Query:
I would like you to help me run MD simulation with the following steps:

1. Retrieve the stable LiTaO3 structure from Materials Project
2. Create a supercell around the size of 100 atoms
3. Use atomate2 with foundation ML forcefield MACE to run Nose-Hoover NVT simulation
   for 2 ps with annealing temperature scheduling 300 to 800 back to 300 Kelvin.
   Use 2 fs timestep and save the trajectory to a ASE traj file.
4. Read the trajectory file and plot the system temperature vs time

> Entering new AgentExecutor chain...
Thought: Do I need to use a tool? Yes
Action: MPStructureRetriever
Action Input: LiTaO3

> Entering new AgentExecutor chain...
Action:
```json
{
 "action": "search_materials_structure__get",
 "action_input": {
 "formula": "LiTaO3",
 "limit": 5,
 "fields": "material_id,structure"
 }
}
```

```
All retrieved structures are saved as Pymatgen Structure JSON files to the following
paths: mp-3666.json, mp-1105280.json, mp-754345.json, mp-1105216.json, mp-
-1105326.json
```

```
> Finished chain.
{'input': 'LiTaO3', 'output': 'All retrieved structures are saved as Pymatgen
Structure JSON files to the following paths: mp-3666.json, mp-1105280.json, mp-
-754345.json, mp-1105216.json, mp-1105326.json'}
Do I need to use a tool? Yes
Action: MPSummaryExpert
Action Input: mp-3666

> Entering new AgentExecutor chain...
Action:
```json
{
  "action": "search_materials_summary__get",
  "action_input": {
    "material_ids": "mp-3666"
  }
}
```Error on search_materials_summary__get: 'fields' must be specified in the query.
Please revise arguments or try smaller request by specifying 'limit' in request
.
```json
{
```



```
"action": "search_materials_summary__get",
"action_input": {
  "material_ids": "mp-3666",
  "fields": "material_id,formula_pretty,composition,nsites,symmetry"
}
}
```

```
[{'nsites': 10, 'composition': {'Li': 2.0, 'Ta': 2.0, 'O': 6.0}, 'formula_pretty': 'LiTaO3', 'symmetry': {'crystal_system': 'Trigonal', 'symbol': 'R3c', 'number': 161, 'point_group': '3m', 'symprec': 0.1, 'version': '2.0.2'}, 'material_id': 'mp-3666'}]
```

```
Action:
'''json
{
  "action": "Final Answer",
  "action_input": "Material ID mp-3666 corresponds to Lithium Tantalate (LiTaO3). It has a trigonal crystal system with space group R3c (number 161) and point group 3m. The structure consists of 10 sites, composed of Li, Ta, and O."
}
'''
```

Finished chain.

```
{'input': 'mp-3666', 'output': 'Material ID mp-3666 corresponds to Lithium Tantalate (LiTaO3). It has a trigonal crystal system with space group R3c (number 161) and point group 3m. The structure consists of 10 sites, composed of Li, Ta, and O.'}
```

Do I need to use a tool? Yes

Action: MPStructureRetriever

Action Input: mp-3666

Entering new AgentExecutor chain...

```
Action:
'''json
{
  "action": "search_materials_structure__get",
  "action_input": {
    "material_ids": "mp-3666",
    "limit": 1,
    "fields": "material_id,structure"
  }
}
'''
```

All retrieved structures are saved as Pymatgen Structure json files to the following paths: mp-3666.json

Do I need to use a tool? Yes

Action: Python_REPL

Action Input:

```
from pymatgen.core import Structure

# Load the structure from the JSON file
structure = Structure.from_file('mp-3666.json')

# Create a supercell to approximately reach 100 atoms
num_atoms = len(structure)
multiplier = int((100 / num_atoms) ** (1/3)) + 1 # Calculate the multiplier for each dimension
```

```

supercell = structure * (multiplier, multiplier, multiplier)

# Save the supercell structure to a file and print the number of atoms
supercell.to(fmt="poscar", filename="supercell.vasp")
print({"supercell_path": "supercell.vasp", "num_atoms": len(supercell)})

```

```

{'supercell_path': 'supercell.vasp', 'num_atoms': 270}

```

```

Do I need to use a tool? Yes
Action: MLFFMDAgent
Action Input: {"structure_path": "supercell.vasp", "forcefield": "MACE", "
simulation_type": "NVT", "temperature_schedule": [300, 800, 300], "
simulation_time": 2, "timestep": 2, "trajectory_file": "trajectory.traj"}Do I
need to use a tool? Yes

```

```

> Entering new AgentExecutor chain...

```

```

Action:
```json
{
 "action": "MLFF MD",
 "action_input": {
 "run_mode": "local",
 "project": "llamp-atomate2",
 "atom_path_or_dict": "supercell.vasp",
 "force_field_name": "MLFF.MACE",
 "time_step": 2,
 "n_steps": 1000,
 "ensemble": "NVT",
 "dynamics": "langevin",
 "temperature": [300, 800, 300],
 "traj_file": "trajectory.traj",
 "traj_file_fmt": "ase",
 "traj_interval": 1
 }
}
```Action:

```

```

2024-05-12 14:42:31,797 INFO Started executing jobs locally
2024-05-12 14:42:31,837 INFO Starting job - Forcefield MD (040866d1-fbcb-4e0b-9044-0
ed3cf9d0eef)
Using Materials Project MACE for \texttt{MACECalculator} with /global/homes/c/
cyrusyc/.cache/mace/5yyxdm76
Using \texttt{float32} for \texttt{MACECalculator}, which is faster but less
accurate. Recommended for MD. Use float64 for geometry optimization.
Default dtype float32 does not match model dtype float64, converting models to
float32.
2024-05-12 14:43:58,683 INFO Finished job - Forcefield MD (040866d1-fbcb-4e0b-9044-0
ed3cf9d0eef)
INFO:jobflow.core.job:Finished job - Forcefield MD (040866d1-fbcb-4e0b-9044-0
ed3cf9d0eef)
2024-05-12 14:43:58,710 INFO Finished executing jobs locally
INFO:jobflow.managers.local:Finished executing jobs locally
{'energy': -2262.60595703125, 'n_steps': 1001}

```

```

Action:
```json
{
 "action": "Final Answer",
 "action_input": "The molecular dynamics simulation was successfully completed. The
 final energy of the system after 1001 steps is -2262.60595703125 eV."
}
```Action:
```json
{
 "action": "Final Answer",
 "action_input": "The molecular dynamics simulation was successfully completed. The
 final energy of the system after 1001 steps is -2262.60595703125 eV."
}
```

> Finished chain.
{'input': '{"structure_path": "supercell.vasp", "forcefield": "MACE", "
  simulation_type": "NVT", "temperature_schedule": [300, 800, 300], "
  simulation_time": 2, "timestep": 2, "trajectory_file": "trajectory.traj"}', '
  output': 'The molecular dynamics simulation was successfully completed. The
    final energy of the system after 1001 steps is -2262.60595703125 eV.}'Do I need
    to use a tool? Yes
Action: Python_REPL
Action Input:

```

```

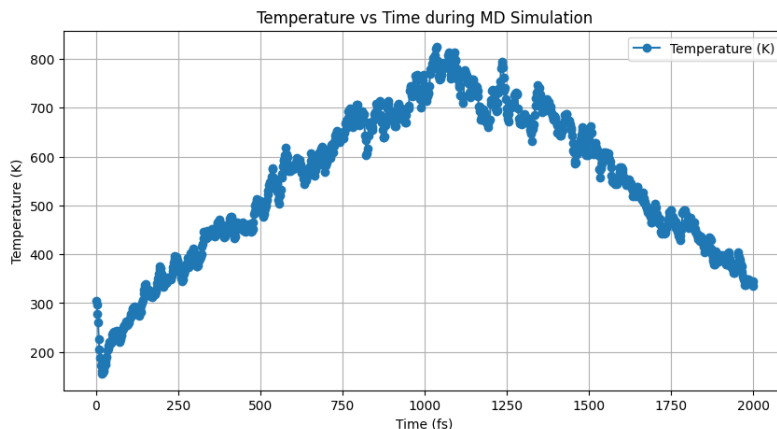
import matplotlib.pyplot as plt
from ase.io import read

# Load the trajectory
trajectory = read('trajectory.traj', index=':')

# Extract temperatures and time steps
temperatures = [step.get_temperature() for step in trajectory]
time_steps = [i * 2 for i in range(len(temperatures))] # Calculate time steps
manually since each step is 2 fs

# Plotting
plt.figure(figsize=(10, 5))
plt.plot(time_steps, temperatures, label='Temperature_(K)', marker='o')
plt.title('Temperature_vs_Time_during_MD_Simulation')
plt.xlabel('Time_(fs)')
plt.ylabel('Temperature_(K)')
plt.grid(True)
plt.legend()
plt.savefig('temperature_vs_time.png')
plt.show()
print({"temperature_vs_time_plot": "temperature_vs_time.png"})

```



C.2 Simulation code generation and execution

Below we present how LLaMP can generate, self-correct, and execute ASE simulation code to calculate bulk modulus of Aluminum.

Generate a script and run ASE EMT calculator to relax 2x2x2 Al supercell and calculate its bulk modulus

Entering new AgentExecutor chain...

To generate a script and run the ASE (Atomic Simulation Environment) EMT (Effective Medium Theory) calculator to relax a 2x2x2 Al supercell and calculate its bulk modulus, we need to write a Python script that uses ASE's functionalities. Here's a step-by-step breakdown of what the script will do:

1. Import necessary modules from ASE.
2. Create an aluminum (Al) supercell.
3. Set up the EMT calculator.
4. Relax the structure using the EMT calculator.
5. Calculate the bulk modulus.

Let's write the script:

```
from ase import Atoms
from ase.build import bulk
from ase.calculators.emt import EMT
from ase.constraints import StrainFilter, ExpCellFilter
from ase.optimize import BFGS
from ase.eos import EquationOfState

# Create an Al supercell
al = bulk('Al', 'fcc', a=4.05, cubic=True)
al = al.repeat((2, 2, 2)) # Repeat the unit cell to create a 2x2x2 supercell

# Set up the EMT calculator
al.set_calculator(EMT())

# Relax the structure
strain_filter = StrainFilter(al)
optimizer = BFGS(strain_filter)
optimizer.run(fmax=0.01)

# Calculate the bulk modulus
```

```

volumes = []
energies = []
for x in [0.98, 0.99, 1.00, 1.01, 1.02]:
    al_copy = al.copy()
    al_copy.set_calculator(EMT())
    cell = al_copy.get_cell()
    al_copy.set_cell(cell * x, scale_atoms=True)
    volumes.append(al_copy.get_volume())
    energies.append(al_copy.get_potential_energy())

eos = EquationOfState(volumes, energies)
v0, e0, B = eos.fit()
eos.plot('al-eos.png')

print(f'Bulk modulus: {B/_kJ}_GPa')

```

Now, let's execute this script using the Python\REPL tool.

Action: Python\REPL
Action Input:

```

from ase import Atoms
from ase.build import bulk
from ase.calculators.emt import EMT
from ase.constraints import StrainFilter, ExpCellFilter
from ase.optimize import BFGS
from ase.eos import EquationOfState
from ase.units import kJ

# Create an Al supercell
al = bulk('Al', 'fcc', a=4.05, cubic=True)
al = al.repeat((2, 2, 2)) # Repeat the unit cell to create a 2x2x2 supercell

# Set up the EMT calculator
al.set_calculator(EMT())

# Relax the structure
strain_filter = StrainFilter(al)
optimizer = BFGS(strain_filter)
optimizer.run(fmax=0.01)

# Calculate the bulk modulus
volumes = []
energies = []
for x in [0.98, 0.99, 1.00, 1.01, 1.02]:
    al_copy = al.copy()
    al_copy.set_calculator(EMT())
    cell = al_copy.get_cell()
    al_copy.set_cell(cell * x, scale_atoms=True)
    volumes.append(al_copy.get_volume())
    energies.append(al_copy.get_potential_energy())

eos = EquationOfState(volumes, energies)
v0, e0, B = eos.fit()

print(f'Bulk modulus: {B/_kJ}_GPa')

```

```

Step      Time           Energy           fmax
BFGS:    0 01:37:31    -0.048066       8.967521
BFGS:    1 01:37:31     1.542253       33.456077
BFGS:    2 01:37:31    -0.154186       1.250352
BFGS:    3 01:37:31    -0.156157       0.259261
BFGS:    4 01:37:31    -0.156246       0.000522
Bulk modulus: 3.923492594026645e-23 GPa

```

The output of the bulk modulus calculation seems to be incorrect because the value is extremely small and not in the expected range for aluminum. This is likely due to a unit conversion error. The ASE package uses eV and Angstroms for energy and length, respectively, and the bulk modulus should be in units of eV/Angstrom³, which can be converted to GPa. The conversion factor from eV/Angstrom³ to GPa is approximately 160.21766208. Let's correct the script to include the proper conversion factor and rerun the calculation.

Action: Python_REPL
Action Input:

```

from ase import Atoms
from ase.build import bulk
from ase.calculators.emt import EMT
from ase.constraints import StrainFilter, ExpCellFilter
from ase.optimize import BFGS
from ase.eos import EquationOfState
from ase.units import kJ

# Create an Al supercell
al = bulk('Al', 'fcc', a=4.05, cubic=True)
al = al.repeat((2, 2, 2)) # Repeat the unit cell to create a 2x2x2 supercell

# Set up the EMT calculator
al.set_calculator(EMT())

# Relax the structure
strain_filter = StrainFilter(al)
optimizer = BFGS(strain_filter)
optimizer.run(fmax=0.01)

# Calculate the bulk modulus
volumes = []
energies = []
for x in [0.98, 0.99, 1.00, 1.01, 1.02]:
    al_copy = al.copy()
    al_copy.set_calculator(EMT())
    cell = al_copy.get_cell()
    al_copy.set_cell(cell * x, scale_atoms=True)
    volumes.append(al_copy.get_volume())
    energies.append(al_copy.get_potential_energy())

eos = EquationOfState(volumes, energies)
v0, e0, B = eos.fit()

# Convert the bulk modulus from eV/Angstrom^3 to GPa
B_GPa = B * 160.21766208

print(f'Bulk modulus: {B_GPa} GPa')

```



```
Step      Time      Energy      fmax
BFGS:    0 01:37:48  -0.048066   8.967521
BFGS:    1 01:37:48   1.542253  33.456077
BFGS:    2 01:37:48  -0.154186   1.250352
BFGS:    3 01:37:48  -0.156157   0.259261
BFGS:    4 01:37:48  -0.156246   0.000522
Bulk modulus: 39.23492594026644 GPa
```

Do I need to use a tool? No

Final Answer: The corrected bulk modulus of the relaxed 2x2x2 Al supercell calculated using the ASE EMT calculator is approximately 39.23 GPa.

Finished chain.